# Nonlinear ferromagnetic resonance in permalloy films: A nonmonotonic power-dependent frequency shift

Y. Khivintsev,[1,*] Bijoy Kuanr,[1] T. J. Fal,[1] M. Haftel,[1] R. E. Camley,[1] Z. Celinski,[1] and D. L. Mills[2]
[1]*Center for Magnetism and Magnetic Nanostructures, University of Colorado at Colorado Springs, Colorado Springs, Colorado 80918, USA*
[2]*Department of Physics and Astronomy, University of California–Irvine, Irvine, California 92697, USA*
(Received 15 October 2009; revised manuscript received 5 January 2010; published 23 February 2010; corrected 5 March 2010)

We present experimental data on the power-dependent shift in the ferromagnetic resonance frequency of permalloy ribbons magnetized in plane. We find the sign of the shift depends on the strength of the applied static magnetic field. For low applied fields, the power-dependent shift is upwards in frequency, while for high fields the mode softens with increasing power. We summarize two theoretical studies that are qualitatively compatible with this result. One is an analytic treatment of very thin films and the second a numerical simulation of a thin rectangular prism.

DOI: 10.1103/PhysRevB.81.054436 PACS number(s): 76.50.+g, 75.40.Gb, 75.50.Bb

## I. INTRODUCTION

The study of ferromagnetic resonance (FMR) in ferromagnets and ferrimagnets has provided us with deep insights into nonlinear physics. In these materials, one can apply sufficient power to drive the precession angle of the spins into the large amplitude regime, where the nonlinear response may be explored. Very soon after FMR was observed in yttrium iron garnet (YIG), it was discovered[1] that the resonance saturated at surprisingly low power. This behavior was explained in a remarkably quantitative manner by Suhl.[2] Moreover, subsidiary absorptions are observed confirming the presence of Suhl's instabilities. An excellent summary of these early studies and related theory can be found in a review article by Patton.[3]

More recently, chaotic behavior has been observed in FMR studies of YIG films.[4] Since the spin Hamiltonian of YIG is known in great detail, it is possible to carry out fully quantitative studies of the chaotic response of these films and compare with theoretical simulations. Theory and experiment are in excellent accord. Also both bright and dark solitons have been observed in feedback rings fabricated from YIG,[5] and chaotic solitary spin-wave pulses have also been produced.[6] Excellent summaries of nonlinear effects in ferromagnetic resonance studies of garnet materials are available.[7,8]

Until recently[9–12] studies of nonlinear phenomena via FMR have been carried out in YIG or in closely related materials. The reason is that their very narrow linewidths allow access to nonlinear response at modest applied microwave power. Nonlinear behavior can also be found in metals for current-driven experiments where the effective damping is significantly reduced through the spin-torque-transfer effect.[13] We have recently developed an experimental approach that allows access to nonlinear phenomena in metallic films where the FMR linewidths are orders of magnitude larger than in the ferrites. We utilize a microstrip geometry with a small cross-sectional area that generates very large oscillating microwave fields. We can attain driving fields as large as 500 Oe compared to the 0.1 Oe realized in standard FMR spectrometers. We can also measure FMR signals over a wide range of frequencies. This opens up for study a much wider range of materials, including metallic ferromagnetic films such as permalloy. In such materials we can explore nonlinear behavior far beyond the threshold limits described by Suhl.

The reason for this large driving field is simple. The Poynting vector, representing the power transmitted per unit area, is proportional to $h^2$. The majority of the energy is contained just under the signal line. Thus, if the power level is constant a reduction in the width of the signal line reduces the area and increases $h$. For the same power level, wider signal lines lead to smaller values of the oscillating $h$ field.

In this paper, we present data obtained through use of the structure just described on the power dependence of the FMR frequency in permalloy ribbons. We find a most striking effect. The sign, and, not just the magnitude, of the power-dependent shift depends on the strength of the applied static magnetic field. For low applied fields, the FMR frequency increases rather than softens with increasing power, whereas for high applied fields the mode softens. It is the case that such a nonmonotonic dependence of the power dependence of the FMR frequency of an infinitely extended thin film was predicted theoretically[14] for the backward volume wave geometry.

In addition to the surprising results described above, we also present an analytical description of the power-dependent shift of the FMR frequency in thin films, and we present numerical studies that illustrate the effect as well. One should note that theoretical analyses of soliton propagation in ferromagnetic films[8] are based on a simple intuitive picture of the origin of the shift; in this picture, the FMR mode only softens with power for all applied Zeeman fields. It is necessary to analytically calculate or numerically study nonlinearities in the equations of motion of the spin system for a sample of finite thickness to obtain a proper description of the power-dependent shift.

## II. EXPERIMENTAL RESULTS

In the experiments, we use a microstrip waveguide structure with a permalloy ribbon placed under the signal line as

 ©2010 The American Physical Society

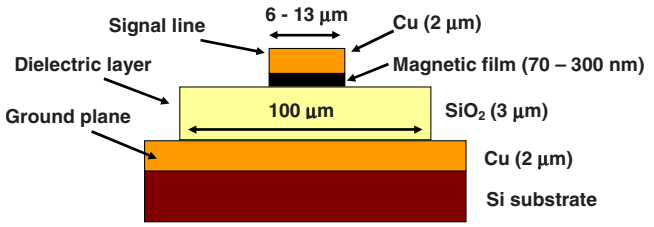


FIG. 1. (Color online) Schematic of the microstrip structure. The thicknesses of the layers used in the experiment are: Cu—2 $\mu$m, permalloy—70 or 300 nm, and $SiO_2$—3 $\mu$m. The width of the signal line in the experiments was 6, 9, or 13 $\mu$m.

shown in Fig. 1. The fabrication was done with magnetron sputtering, photolithography, and ion etching. First a 2-$\mu$m-thick Cu film was grown on a Si substrate. The remaining depositions, including 3 $\mu$m of $SiO_2$, 70 or 300 nm of permalloy, and then 2 $\mu$m of Cu, were carried out through a shadow mask. The microstrip waveguide with a 6-, 9-, or 13-$\mu$m-wide signal line was then created using photolithography and ion etching.

Microwave characterization of the structure was done using a vector network analyzer along with an external power amplifier and a probe station. Measurements were carried out in the 2–28 GHz frequency range with input power up to +33 dBm (2 Watts). An external static magnetic field, $H$, was applied along the long axis of the waveguide structure. A transverse microwave pumping field, $h_d$, was applied parallel to the surface and perpendicular to the static field. The $S$ parameters as a function of frequency were measured. The data were analyzed in order to extract the frequency dependence of the FMR absorption (effectively the imaginary part of the microwave magnetic susceptibility of the structure).

Typical experimental data are presented in Fig. 2 for a structure with a 70-nm-thick Py film and a signal line of width 6 $\mu$m. Figures 2(a) and 2(b) show absorption peaks at different input powers for low and high static applied magnetic fields. Figures 2(c) and 2(d) show the influence of input power on peak position, defined as the absorption maximum, and the magnitude of the FMR peak for different applied fields. One can see the FMR frequency shift with increasing power. It can be positive or negative, depending on the bias field; at low fields the shift is positive, and at high fields the shift becomes negative. The positive as well as the negative frequency shifts always occur with the FMR saturation effect [Fig. 2(d)], which we associate with the spin-wave parametric instability.

We studied a variety of structures with 300 nm of permalloy and with signal lines of width of 6, 9, and 13 $\mu$m. Typical results are presented in Figs. 3 and 4 for the structure with a 9-$\mu$m-wide signal line. Figure 3 shows FMR absorption as a function of frequency for different static fields and different power levels. The main results seen in Fig. 2 are present here as well. At low static fields, the frequency shifts upward as the power level is increased by up to about 2 GHz. At higher static fields there is a downward shift in frequency as power is increased, and the frequency shift is much smaller in magnitude. We note that in addition to the FMR absorption peak in these spectra, there is an additional peak at higher frequencies which is associated with subsidiary

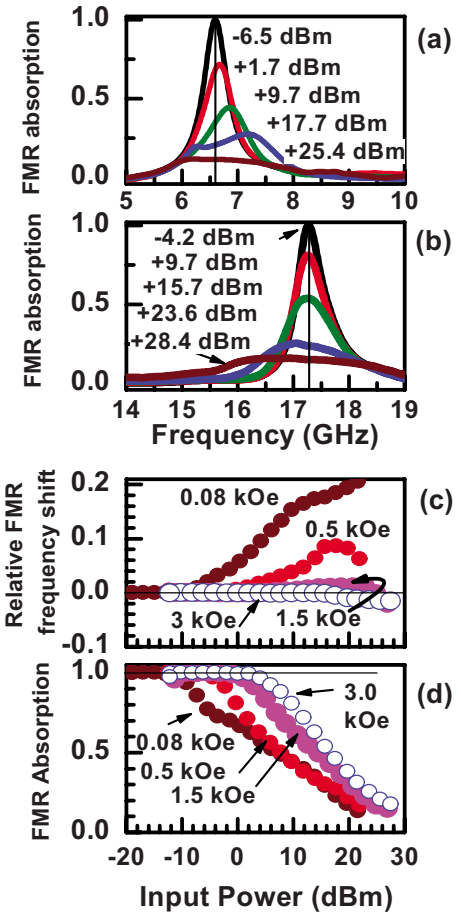


FIG. 2. (Color online) Experimental data: (a) and (b) are normalized FMR absorption versus frequency for low $H$=0.5 kOe and high $H$=3 kOe applied magnetic fields, respectively, at different power levels. (c) and (d) show the relative FMR frequency shift and normalized FMR absorption as a function of input power for different bias fields.

absorption.[2] We have also made measurements on a similar structure which contained a 100 nm Fe film with the same general results.

Changing the width of the signal line does not change the general features noted above. However, it does change the power thresholds for the transition to nonlinear behavior. We take this transition point as the power level at which the FMR absorption amplitude begins to decrease. For example, the lowest power thresholds for the 6-, 9-, and 13-$\mu$m-wide permalloy ribbons (70 nm thick) are approximately −11, −5, and −4 dBm, respectively. This is in agreement with the discussion presented earlier showing that, for a fixed power level, the $h$ field decreases as the signal line is made wider. Thus to obtain the same critical threshold field, $h_{thr}$, one needs to increase the power level.

Figure 4 summarizes the results for the structure with the 300 nm permalloy film and with a 9-$\mu$m-wide signal line. The upper panel shows the relative changes in the FMR frequency; the lower panel shows the change in the FMR absorption amplitude. Here the filled symbols represent the low static field values (0.08–0.5 kOe) and the open symbols show the results for the higher static field values (1–3 kOe).

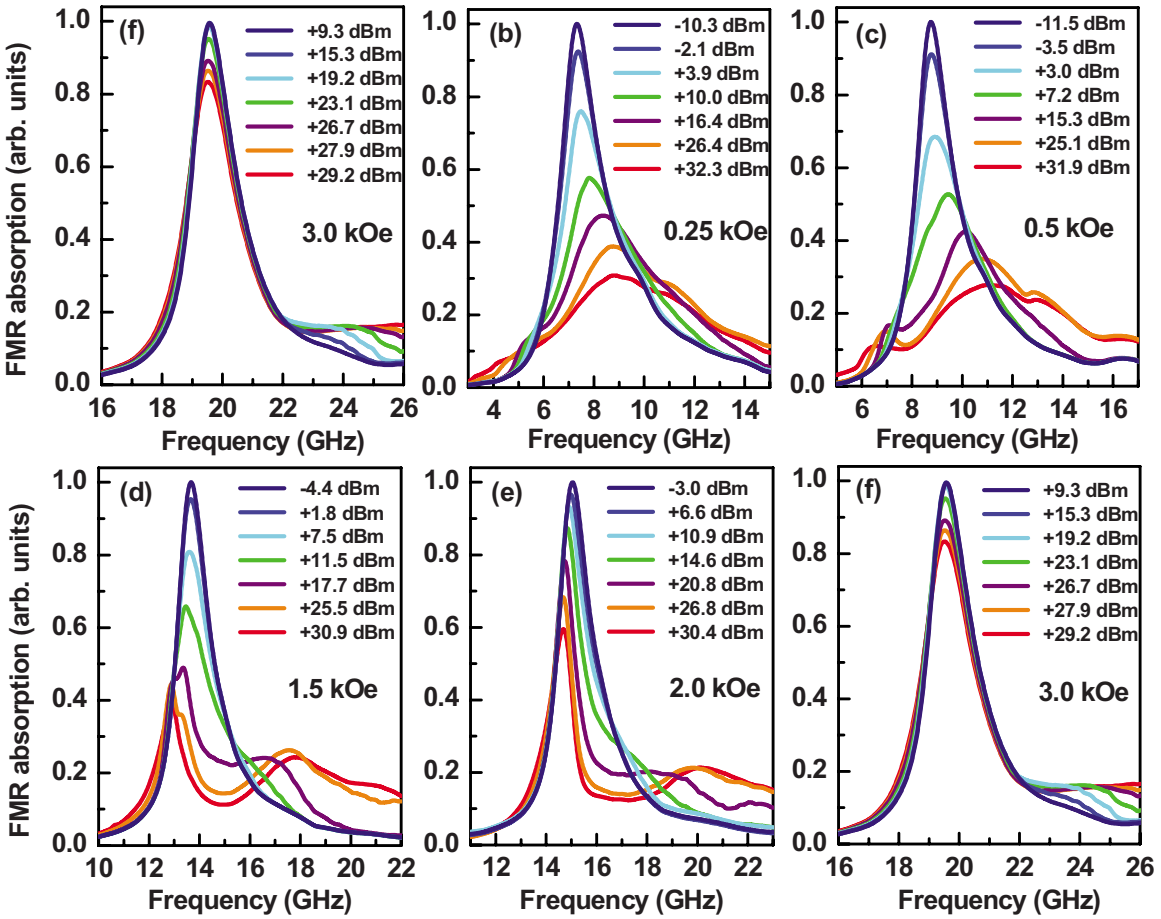


FIG. 3. (Color online) Experimental data for the structure with 300-nm-thick permalloy and a 9-$\mu$m-wide signal line: (a)–(f) are the normalized FMR absorption versus frequency for different values of the applied magnetic field at different power levels.

The difference between the two cases is particularly noticeable in the frequency-shift data.

We do not observe any frequency shift (with accuracy of 35 MHz) associated with possible heating effects at high power. To check for this, we made the following test. Measurements were carried out by increasing the input power. After a measurement at high power, under conditions where the frequency shift is positive, we decreased the power and made a control measurement at the lowest power. If the sample had been heated, one would expect a negative FMR frequency shift for the control measurement. However, we did not observe any substantial shift for this case. Figure 5

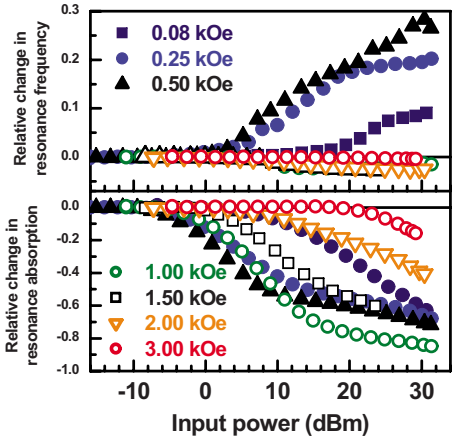


FIG. 4. (Color online) Summary of experimental results for the 300-nm-thick permalloy sample with a 9-$\mu$m-wide signal line: (a) and (b) show the relative FMR frequency shift and normalized FMR absorption as a function of input power for different bias fields.

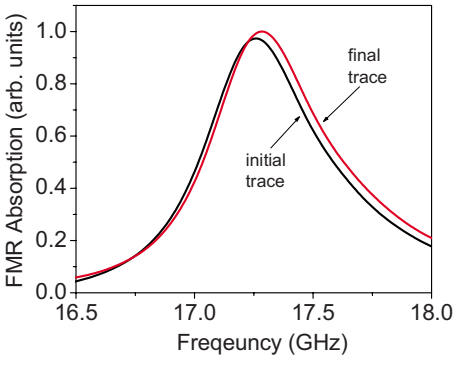


FIG. 5. (Color online) FMR absorption as a function of frequency for low-power level (linear regime). The initial trace shows the absorption before any high-power measurements. The final trace shows the absorption, again at low power, after the high-power measurements were taken. The difference between the two traces, 35 MHz, is much smaller than the measured shifts at high power.

shows the FMR absorption for the 70 nm Py film with a signal line of width 6 $\mu$m at low power, −12.2 dBm (linear regime), both before and after applying high power. There is a very small shift, 35 MHz, which is probably due to a small drift in the value of the magnetic field with time. We made similar measurements on other structures and the measured shifts were 35 MHz or less.

One can estimate the maximum temperature increase of the system in a simple way. At resonance the magnetic system effectively absorbs most of the microwave energy. This raises the temperature of the system. We assume, for example, that the increase in temperature is 10 K in the signal line (i.e., Cu overlayer and permalloy), and that this creates a temperature difference of 10 K across the $SiO_2$ which is 3 $\mu$m thick. Using the heat-transfer formula

$$q = k\frac{dT}{dx} \tag{1}$$

with the heat-transfer coefficient of 1.7 W m$^{-1}$ K$^{-1}$,[15] one finds that $q$ is $5\times10^6$ W m$^{-2}$. Using the area of the signal line, $6\times10^{-8}$ m$^2$, the total power that would be transmitted across the $SiO_2$ is 0.3 W. The maximum power absorbed is about 1 W, however, this occurs only a small fraction of the measuring time, less than 10%, as the frequency is scanned across its entire range. Thus all of the power absorbed by the ferromagnet is transferred to the ground plane and substrate if the temperature in the signal is 10 K above ambient. This clearly limits the maximum temperature increase in the ferromagnet to about 10 K. Such a temperature increase would result in a nearly immeasurable decrease in the frequency of approximately 4 MHz.

## III. THEORETICAL CONSIDERATIONS

We comment on the origin of the frequency shifts. In a macrospin model and in the linear regime, one expects the frequency to always decrease as the power is increased. The reason for this can be understood intuitively by the following argument. In the linear limit the FMR frequency, $f$, is given by the well-known Kittel formula. For a bar geometry with magnetization in the $z$ direction the result is

$$f = \gamma\sqrt{[H + 4\pi M_z(N_x - N_z)][H + 4\pi M_z(N_y - N_z)]}. \tag{2}$$

Here $\gamma$ is the gyromagnetic ratio, $H$ is the applied field, $N_x$, $N_y$, and $N_z$, are demagnetizing factors, and $M_z$ is the $z$ component of magnetization. An increase in driving power is expected to increase the precession angle, thus reducing $M_z$ and reducing the frequency.[8] In fact, this behavior is seem in the experiments when the applied field is large and the magnetic system is all nearly aligned with the external field, i.e., the system is close to that of a macrospin.

However, the positive frequency shift seen in the experiment is incompatible with this simple picture; for the present geometry only a softening with increased power would be expected for all external magnetic fields. We conclude that the macrospin model is not appropriate at low fields and that spatial variations in the magnetization play an important role. Below we describe our theoretical studies that display a sign change in the field dependence of the power-dependent FMR frequency similar to the experimental data just presented.

We first consider an in-plane magnetized thin film of thickness $D$ and examine spin waves with wave vector $k$ in the regime $kD \ll 1$. We have derived the power dependence of the spin-wave frequency for two propagation directions, parallel to the magnetization, the so-called magnetostatic backward volume wave (MSBVW) geometry, and perpendicular to the magnetization, the magnetostatic surface wave (MSSW) geometry.[3] The spins precess in the presence of a static applied magnetic field $H_0$ in combination with the dipolar field $\vec{h}_{\rm dip}(\vec{r},t) = -\vec{\nabla}\varphi_M(\vec{r})\exp[-i\omega t]$ generated by the spin motions. We perform a perturbation theoretical analysis of the nonlinear equations of motion and associated boundary conditions by expanding all quantities in powers of the amplitude of the spin motions. Thus we write

$$\varphi_M(\vec{r}) = \varphi_M^{(1)}(\vec{r}) + \varphi_M^{(2)}(\vec{r}) + \varphi_M^{(3)}(\vec{r}) + \cdots \tag{3}$$

and similarly for the transverse components of spin amplitude $\{m_\alpha(\vec{r})\}$. Here $\varphi_M^{(i)}(\vec{r})$ is proportional to the amplitude of the transverse magnetization to the power $i$. To find the lowest order power-dependent shift to the spin-wave frequency in a perturbation calculation, one must take the quantities $\{\varphi_M^{(2)}(\vec{r}), m_\alpha^{(2)}(\vec{r})\}$ to second order and $\{\varphi_M^{(3)}(\vec{r}), m_\alpha^{(3)}(\vec{r})\}$ to first order. The former, viewed in microscopic language, correspond to the three magnon interaction taken to the second order of perturbation theory and the latter the four magnon interaction taken to first order. These two pieces contribute to the same order in the amplitude of the spin motion. The analysis is very lengthy and will be described elsewhere.[14]

For the MSBVW case, we find that when $kD \ll 1$ the spin-wave frequency is given by

$$\Omega_\parallel^2(k) = B_0H_0 - 2\pi M_S H_0 kD - \pi[m_\parallel^{(0)}/M_S]^2(M_S/B_0)(B_0 + H_0)(H_0 - \pi M_S) \tag{4}$$

and for the MSSW geometry

$$\Omega_\perp^2(k) = B_0H_0 + 8\pi^2 M_S^2 kD - (3\pi/2)[m_\parallel^{(0)}/M_S]^2 M_S H_0(B_0 + H_0)/B_0. \tag{5}$$

In these expressions, $M_S$ is the saturation magnetization, $B_0 = H_0 + 4\pi M_S$, and $m_\parallel^{(0)}$ is the component of the dynamic magnetization parallel to the film surfaces. We see that for propagation parallel to the magnetization, for low applied fields the spin wave stiffens with power, whereas when $H_0 > \pi M_S$ the mode softens with power. In the MSSW geometry we realize only softening. The physical origin in the difference in the formulas for the two cases is that in the MSBVW geometry, the spin-wave eigenvector has its maximum in the center of the film, so saturation first appears near the center of the film as power is increased. In contrast, for the MSSW geometry, there are maxima in the eigenvectors at the film surfaces, so saturation first occurs near the surfaces. Both power-dependent corrections are independent of wave vector in the limit considered. Formally, the power-dependent corrections are nonanalytic in the wave vector as $k \to 0$, in that they depend on the direction in which the wave vector approaches zero. Such behavior is encountered com-

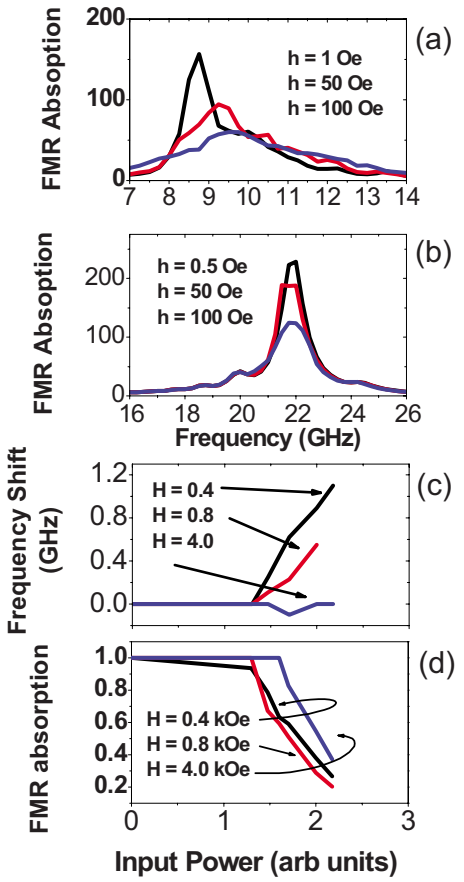


FIG. 6. (Color online) Theoretical results: (a) and (b) are FMR absorption vs frequency for low $H_0$=0.5 kOe and high $H_0$ =2 kOe applied magnetic fields, respectively, at different power levels. (c) and (d) show the relative FMR frequency shift and maximum normalized FMR absorption as a function of power for different Zeeman fields. Because of the significant computational demands, these calculations were done with large cells, $15\times15$ nm$^2$ in the plane of the sample. Limited sets of calculations were done with much smaller cells ($8\times8$ nm$^2$) and show the same general behavior.

monly in the presence of long-ranged dipolar couplings between the spins. For instance, the group velocity of spin waves in linear theory is independent of the magnitude of the wave vector when $k\rightarrow0$, but both its sign and magnitude depend on the direction of approach to the origin.

In the experiments, the spin waves propagate parallel to the magnetization for the in plane-magnetized samples. However, the change in sign of the experimentally observed power-dependent shift occurs somewhat below $\pi M_S$. The films in the experiment have finite width $W$, of course. In such ribbons, in the magnetostatic limit the edges of the ribbon act as pinning centers even in the absence of surface anisotropy.[16] The spin wave that propagates down the film may be regarded, to good approximation, as an appropriate superposition of two plane waves with wave vectors in the plane of the film $\vec{k}_\parallel=\hat{z}k\pm\hat{x}(\pi/W)$, i.e., as a superposition of two plane waves each with wave vector canted away from the direction $\hat{z}$ of the magnetization. Since we find only softening with power for the MSSW case, it is plausible that for waves that propagate with wave vectors canted with respect to the magnetization, the crossover from power-induced stiffening to softening occurs below $\pi M_S$.

We have also carried out numerical simulations of the power-dependent FMR frequency for model samples in the form of rectangular prisms. We proceed by integrating in time the Landau Lifschitz Gilbert equation

$$\frac{\partial\vec{M}}{\partial t}=-\frac{|\gamma|}{1+\alpha^2}\left[\vec{M}\times\vec{H}_{\text{eff}}-\frac{\alpha}{M_S}\vec{M}\times(\vec{M}\times\vec{H}_{\text{eff}})\right], \quad (6)$$

where $\vec{H}_{\text{eff}}$ includes the Zeeman field $H_0$, the exchange field, static, and dynamic dipolar fields and finally the microwave driving field which has frequency $\Omega$.

Numerical results for FMR in a 100-nm-thick, 1920-nm-long, and 960-nm-wide Py sample are presented in Fig. 6. We have calculated power absorbed by evaluating the integral

$$P=\frac{1}{T}\left\{\int_0^T dt(d\vec{M}^{(\text{tot})}(t)/dt)\cdot\vec{h}_{\text{ext}}(t)\right\}. \quad (7)$$

There are issues in the study of the nonlinear response. First there are initial transients at each new frequency, and one must wait for these to die down before calculating the absorption. Second, because the system is nonlinear, not all relevant behaviors are evident in a single period. One must thus collect data over many periods after transients die out. We have averaged over both 60 and 200 periods; the differences are generally small.

Figures 6(a) and 6(b) present absorption as a function of frequency for different oscillating field $h$ values. It is not possible to make a direct comparison with the experimental data because the dimensions of the structure are not known exactly and the wave attenuates as it propagates so the value of $h$ decreases along the waveguide. As a guide, however, we note that the power levels of 3.6, 19.3, and 31.2 dBm correspond to approximate field values of 10, 80, and 250 Oe for a 9-$\mu$m-wide signal line.

Qualitative agreement between theory and experiment is quite good. We clearly see the upward shifts in the FMR frequency for small applied magnetic fields, and the softening at large fields. The quantitative agreement is also reasonable. The frequency shifts in the experiment are on the order of up to 2 GHz, at for low static fields, and same values are found in the numerical simulation.

We note that in our numerical studies the ground state differs for high and low fields. For high fields the structure is a "flower state[17]" where the magnetic configuration is nearly uniformly magnetized while for lower fields it is an "$s$ state" where there has been an edge-nucleated transition and the spins at the edges are nearly parallel to the edge rather than perpendicular as in the high-field case.[18] In the analytic study of the infinitely extended thin film, the ground state is uniformly magnetized always. Also in the finite sample in our simulations, in addition to extended standing wave modes, one has edge and corner modes which mix in with FMR mode with increasing power. The edge and corner modes often have frequencies well below the FMR mode. The presence of such modes and their role in the power-dependent

shifts is not incorporated in the infinite extended film study, of course.

## IV. SUMMARY

In this paper, we have described an approach which allows us to study nonlinear effects in permalloy films. For in-plane magnetized films and for small static magnetic fields, the FMR frequency increases with power, whereas in high applied fields, frequency softening is observed. These results are in qualitative agreement with an analytic study of power-dependent frequency shifts of long-wavelength spin waves in infinitely extended thin ferromagnetic films and in semiquantitative agreement with the results of numerical simulations of the nonlinear response of thin rectangular prisms.

## ACKNOWLEDGMENTS

This work was supported by the ARO (Grant No. W911NF-04-1-0247) and NSF (Grant No. DMR 0907063).

*On leave from Kotel'nikov SBIRE RAS, Saratov 410019, Russia.

[1] N. Bloembergen and R. W. Damon, Phys. Rev. **85**, 699 (1952).
[2] H. Suhl, Phys. Rev. **101**, 1437 (1956); J. Phys. Chem. Solids **1**, 209 (1957).
[3] Carl E. Patton, Phys. Rep. **103**, 251 (1984).
[4] R. D. McMichael and P. E. Wigen, *Nonlinear Phenomena and Chaos in Magnetic Materials*, edited by P. E. Wigen (World Scientific, Singapore, 1994), p. 167.
[5] B. A. Kalinikos, N. G. Kovshikov, and C. E. Patton, Phys. Rev. Lett. **80**, 4301 (1998).
[6] M. Wu, B. A. Kalinikos, and C. E. Patton, Phys. Rev. Lett. **95**, 237202 (2005).
[7] *Nonlinear Phenomena and Chaos in Magnetic Materials*, edited by P. E. Wigen (World Scientific, Singapore, 1994).
[8] S. O. Demokritov, B. Hillebrands, and A. Slavin, Phys. Rep. **348**, 441 (2001).
[9] V. E. Demidov, U.-H. Hansen, and S. O. Demokritov, Phys. Rev. Lett. **98**, 157203 (2007).
[10] T. Gerrits, P. Krivosik, M. L. Schneider, C. E. Patton, and T. J. Silva, Phys. Rev. Lett. **98**, 207602 (2007).
[11] M. Yan, P. Vavassori, G. Leaf, F. Y. Fradin, and M. Grimsditch, J. Magn. Magn. Mater. **320**, 1909 (2008).
[12] H. M. Olson, P. Krivosik, K. Srinivasan, and C. E. Patton, J. Appl. Phys. **102**, 023904 (2007).
[13] C. T. Boone, J. A. Katine, J. R. Childress, V. Tiberkevich, A. Slavin, J. Zhu, X. Cheng, and I. N. Krivorotov, Phys. Rev. Lett. **103**, 167601 (2009).
[14] D. L. Mills (unpublished).
[15] O. A. Jaramillo, G. Huelsz, and J. A. del Rio, J. Phys. D **35**, 95 (2002).
[16] R. Arias and D. L. Mills, Phys. Rev. B **72**, 104418 (2005).
[17] M. E. Schabes and H. Neal Bertram, J. Appl. Phys. **64**, 1347 (1988).
[18] W. Rave and A. Hubert, IEEE Trans. Magn. **36**, 3886 (2000).